C-10-5

REMOTE SENSING OF RAINDROP SIZE DISTRIBUTIONS FROM MICROWAVE SCATTERING MEASUREMENTS

Y. FURUHAMA and T. IHARA
Radio Research Laboratories, Koganei-shi, Tokyo 184, JAPAN

INTRODUCTION

Precipitation affects on microwave propagation through the atmosphere. Interaction between a single raindrop and radio wave is made clear theoretically and experimentally. But the drop size in a real rainfall is never uniform and is randomly distributed. Therefore, in order to predict the rain effects on the microwave propagation through the atmosphere, it is essentially important to elucidate the drop size distribution.

In this paper, a new method is proposed to probe raindrop size distribution in the air. Amplitude and phase variations of forward scattering due to rain are measured in phase-locked multichannel experimental propagation system setting up horizontally. We consider that the system uses four coherent waves of 1.7, 11.5, 34.5, and 80.0 GHz signals generated in a single crystal oscillator in order to take not only level measurements but also differential phase shift measurements between two of those frequencies. These data constitute the Fredholm integral equation of the first kind whose unknown function is raindrop size distribution. The equation is calculated numerically by the inversion technique of Backus and Gilbert [1]. The inversion technique is then applied to computer simulated data to recover drop size distribution. This example indicates that the distribution can be recovered at selected points without using assumptions about the shape of the distribution.

MICROWAVE WEIGHTING FUNCTIONS

We assume uniform rainfall over the multichannel experimental propagation system. Then, an effective propagation constant k is given as follows [2],

$$k = k_0 + (2\pi/k_0)\int_0^{a_m} f(a)n(a)da \qquad (1)$$

where k_0 is propagation constant in a clear day, a_m for the maximum raindrop size, f(a) for a forward scattering amplitude, n(a) for an average raindrop size distribution over the path. Attenuation and phase shift due to rain are derived from the imaginary and real parts of Eq.(1), respectively. Experimentally, attenuation X due to rain are determined for the reference level of a clear day and phase shift due to rain is measured as a differential phase shift Y between two frequencies. Then, Eq.(1) can be written as follows,

$$g_i = \int_0^{a_m} K_i(a)n(a)da, \qquad i = 1, 2, 3, \cdots, 6 \quad (2)$$

where, for i = 1, 2, 3, $g_i = X_i k_{0i}/2\pi$, $K_i(a) = -\mathrm{Im}[f_i(a)]$, and for i = 4, 5, 6, $g_i = Y_i k_{0i}/2\pi$, $K_i(a) = \mathrm{Re}[f_i(a) - q_i^2 f_0(a)]$, with $q_4 = 11.5/1.7$, $q_5 = 34.5/1.7$, $q_6 = 80.0/1.7$, and $f_0(a)$ is for the frequency of 1.7 GHz. The kernel $K_i(a)$'s are the microwave weighting functions. The problem is to calculate Eq.(2) with respect to n(a) numerically, because g_i's are the

measured values and $K_i(a)$'s are the given functions. Although there are several inversion methods of Eq.(2), we adopt Backus-Gilbert inversion technique which does not require a trial distribution of n(a). The method can be found in the reference of [1], [3].

Next, for demonstrating the effectiveness of application of Backus-Gilbert inversion technique to determination of the distribution, we introduce the following type of path-averaged raindrop size distribution,

$$n(a) = N_0 \exp(-2\Lambda a) \tag{3}$$

where $\Lambda = AR^{-B}$, R is rainfall rate (mm/h), and parameters of N_0, A, and B are listed in Table 1 for Marshall and Palmer [4], and Joss et al. [5] distributions. Then, the integrand of Eq. (2) is expressed as follows,

$$K_i(a)n(a) = N_0 K_i \exp(-2\Lambda a). \tag{4}$$

The value of the term $\exp(-2\Lambda a)$ plays a predominant role in Eq.(4) and the term comes out commonly for an usual rainfall. Therefore, we compute modified kernel $K_i(a)\exp(-2\Lambda a)$ instead of kernel itself $K_i(a)$ for the convenience of numerical comparison. Forward scattering amplitudes $f_i(a)$ depend not only on probing frequencies and radius of raindrop size, but also on the shape of drop size and temperature. In the following computation, spherical drop size is assumed and the refractive index of water at 20° C is used. Fig. 1 shows modified weighting functions of $K_i(a)\exp(-2\Lambda a)$ for assuming Joss et al.(wide spread) distribution and rainfall rate R = 25 mm/h. The locations of maxima for amplitude and phase curves go to smaller drop size with increase of the probing frequencies.

AVERAGING KERNEL

We compute the values of averaging kernel from 6 weighting functions as shown in Fig. 1 under the assumption that amplitude and phase difference errors are 0.71 dB and 10°, respectively, and propagation distance is 3 km. Fig. 2 shows those values at diameters of 1, 2, and 3 mm. In the ideal case, these curves tend to δ -functions at each diameter. Fig. 3 shows trade-off curves for 6 measurements under the measurement errors. Spread expresses the amount of resolution inherent in the set of weighting functions $K_i(a)$ and relative error is connected with measurement errors of g_i. Improvement in accuracy (reduction in variance) is achieved only by degrading the resolution (increasing the spread), vice versa. The case of Fig. 2 corresponds to one specified point on each curve in Fig. 3.

INVERSION OF SIMULATED DATA

Joss et al.(wide spread) distribution is chosen to check the results of the previous section using simulated measurements. The simulated measurements at three frequencies of 11.5, 34.5, and 80.0 GHz are made through Eq.(2). Amplitude and phase errors are 0.71 dB and 10°, respectively. In Fig. 4, inferred raindrop size distribution functions (dots) at 5 radii from those 6 measurements show good agreement with the true distributions (dotted lines). Vertical bars show errors which come from the measurement errors and incompleteness inherent to the weighting functions.

CONCLUDING REMARKS

Selection of probing frequencies is the most important

parts in this remote sensing of raindrop size distribution. Although these most appropriate frequencies can be selected from studying the characteristics of averaging kernels at various radii, four frequencies used here is not selected from this point of view, but selected from the reason why experimental propagation system for those frequencies are available in our Laboratory. Experimental test of this method is expected to be done hereafter.

This inversion technique of Backus-Gilbert has the principal advantages that definite statements can be made about the achievable resolution and accuracy for a given set of measurements and a priori assumptions about the shape of the distribution is not required. The later fact is useful for remote sensing of drop size distribution of artificial precipitation whose spectrum of drop size is not log-linear as given by Eq.(2), but line spectrum. Extension of this method to the deformed raindrop has the possibility of remote sensing of the canting angle distribution, which has close connection with the degradation of cross-polarization discrimination.

REFERENCES

[1] G. Backus and F. Gilbert, Trans. Roy. Soc. London, 266(1173) pp. 123-192(1970).

[2] H. C. Van deHulst, "Light scattering by small particles", p. 33, John Wiely & Sons, New York(1957).

[3] E. R. Westwater and A. Cohen, Appl. Opt., 12(6), pp. 1340-1348(1973).

[4] J. S. Marshall and W. M. Palmer, J. Meteor., 5, pp.165-166 (1948).

[5] J. Joss, J. C. Thams, and A. Waldvogel, Proc. Intern. Conf. Cloud Phys., Toronto, Canada, pp. 359-373(1968).

Table 1

Distribution		$N_0 (m^{-3}mm^{-1})$	A	B
Marshall and Palmer		8000	4.1	0.21
Joss et al.	drizzle	30000	5.7	0.21
	wide spread	7000	4.1	0.21
	thunderstorm	1400	3.0	0.21

FIGURE CAPTIONS

Fig. 1 Modified weighting functions $K_i(a)\exp(-2\Lambda a)$ for multispectral scattering. Solid lines are for amplitude variations and broken lines are for differential phase shift.

Fig. 2 Averaging kernels at diameters of 1, 2, and 3 mm constructed from 6 modified weighting functions $K_i(a)\exp(-2\Lambda a)$. Amplitude and phase errors assumed to be 0.71 dB and 10°, respectively. Propagation distance is 3 km.

Fig. 3 Error-spread trade-off curves for 6 measurements at rainfall rate 25 mm/h.

Fig. 4 Inferred raindrop size distribution function at 5 radii from 6 simulated measurements assuming Joss et al.(wide spread) raindrop size distribution. Amplitude and phase errors are 0.71 dB and 10°, respectively, trade-off curve is for θ = 20°. Dots denote inferred values, solid lines denote error bars, and dotted lines denote true distributions.

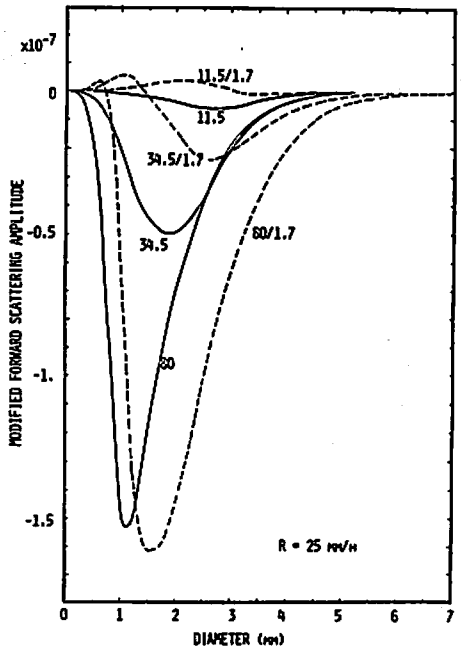

Fig. 1

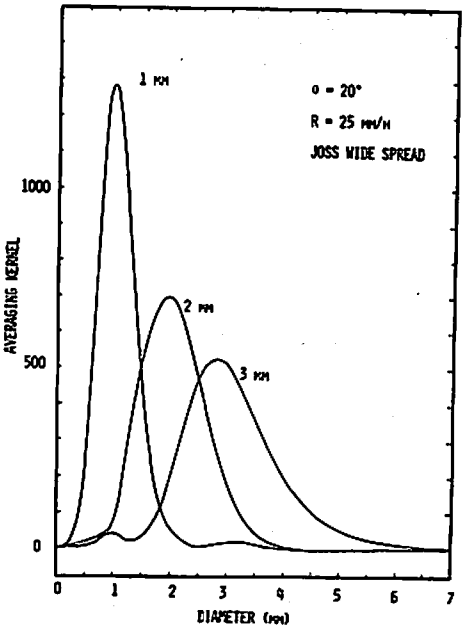

Fig. 2

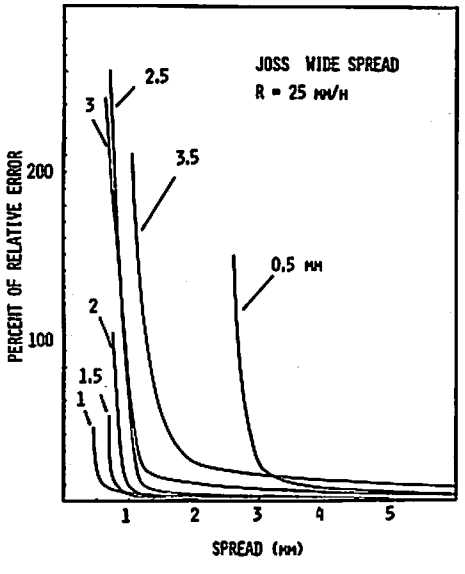

Fig. 3

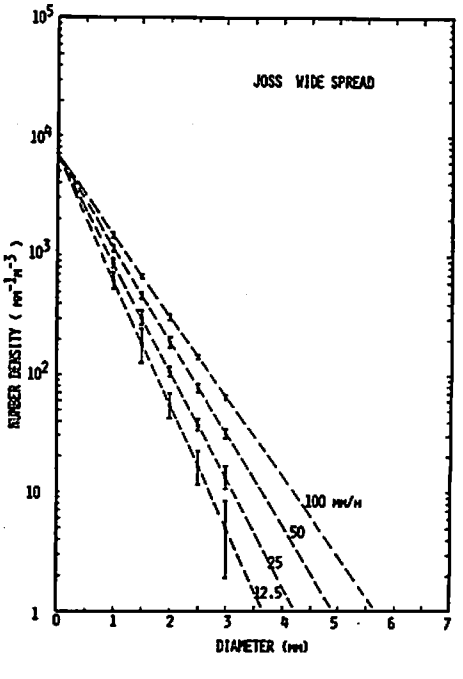

Fig. 4